Evaluation of the structure–activity relationship of flavonoids as antioxidants and toxicants of zebrafish larvae

Yau-Hung Chen [a,*], Zhi-Shiang Yang [a], Chi-Chung Wen [b], Yeong-Sheng Chang [a], Bo-Cheng Wang [a,*,1], Chih-Ang Hsiao [a], Tzenge-Lien Shih [a,*,2]

[a] Department of Chemistry, Tamkang University, Tamsui 25137, New Taipei City, Taiwan
[b] Department of Mathematics, Tamkang University, Tamsui, Taiwan

ARTICLE INFO

ABSTRACT

The antioxidant ability of an array of commercially available flavonoids was evaluated on the larvae of the zebrafish model organism, in order to find flavonoids with lower toxicities and higher radical oxygen-scavenging properties than flavone. Among the flavonoids tested, chrysin and morin possessed higher reactive oxygen species (ROS)-scavenging rates (−99% and −101%, respectively) and lower toxicity ($LD_{50} > 100$ ppm). Zebrafish fins in the UVB + chrysin group were 6.30 times more likely to grow to normal fin size than those in the UVB-only control group, while zebrafish fins in the UVB + morin group were 11.9 times more likely to grow to normal fin size than those in the UVB-only control group. These results were analysed by the QSAR method and were in accordance with predicted values. A new 4′-fluoroflavone was synthesised. The ROS-scavenging rate of 4′-fluoroflavone was −54%, which corresponds well with the predicted value (−48%). We propose that a combination of QSAR prediction and the zebrafish model organism is efficient for evaluating new flavonoids.

© 2012 Elsevier Ltd. All rights reserved.

1. Introduction

Flavonoids are a group of plant polyphenols and are widely present in many plants, including edible fruits and vegetables (Harborne & Williams, 2000; Heim, Tagliaferro, & Bobilya, 2002; Lee, Kim, Kang, & Cho, 2007). Most flavonoids possess antioxidant activities. For example, flavone and 3,4′-dihydroxyflavone can suppress reactive oxygen species (ROS) that are generated by UVB radiation (Lee, Kang, Kim, Lee, & Cho, 2005; Tsai et al., in press). In addition, baicalein (5,6,7-trihydroxyflavone) can suppress ROS and protect cardiomyocytes from lethal oxidant damage (Shao et al., 1999). The ROS-scavenging abilities of flavonoids give them beneficial effects, such as anti-inflammatory, neuroprotective, cardioprotective and UVB-protective activities (Chirumbolo, 2010; Lee et al., 2007; Mazur, Bayle, Lab, Rock, & Rayssiguier, 1999; Ono et al., 2005; Tsai et al., in press).

Structurally, flavonoids are known to have a diphenylpropane (C6C3C6) skeleton. The different ROS-scavenging activities of various flavonoids have been suggested to be dependent on the number and positions of the hydroxyl (OH) groups on their skeletal

carbons (Havsteen, 2002; Lee et al., 2007). For instance, 3′,4′-dihydroxyflavone suppresses the generation of ROS in human HaCaT keratinocytes induced by UVB treatment (Lee et al., 2007). However, another structurally related compound, 3-hydroxyflavone, enhances the generation of intracellular ROS (Lee et al., 2007). Therefore, the structure–activity relationships (SAR) of flavonoids have become an important area of study.

We have previously used a zebrafish model in a series of time- and dose-dependent flavonoid (flavone, flavanone, and chalcone) exposure experiments. Our results showed that flavones have the highest chemoprotective effects against UVB-induced cytotoxicity (Tsai et al., in press). Quantitative structure–activity relationships (QSAR) have frequently been used to determine the correlations between the biological activities and the physicochemical properties of various compounds (Chang, Yang, & Wang, 2010; Liao et al., 2006). Due to the broad spectrum of biological effects of flavonoids, they have become one of the most popular subjects for QSAR studies. In this study, the ROS-scavenging activities of 15 commercially available flavonoids that possessed various hydroxyl groups or other substituents were evaluated by the QSAR method. In addition to the flavonoids, a unique 4′-fluoroflavone was also synthesised, based on a QSAR prediction, and compared to the commercially available flavonoids used in this study. The results of this study will enable us to synthesise other novel flavone derivatives that have lower toxicities and higher antioxidant activities in the future.

* Corresponding author. Tel.: +886 2 2621 5656x3009; fax: +886 2 2620 9924.
  E-mail addresses: yauhung@mail.tku.edu.tw (Y.-H. Chen), bcw@mail.tku.edu.tw
(B.-C. Wang), tlshih@mail.tku.edu.tw (T.-L. Shih).
  [1] Tel.: +886 2 2621 5656x2438.
  [2] Tel.: +886 2 2621 5656x2437.

2. Materials and methods

2.1. Fish embryos

Zebrafish of the AB strain were maintained at approximately 28.5 °C on a 14-h light and a 10-h dark photoperiod. The procedures for zebrafish culture and embryo collection used in this study have been described previously (Chen, Lee, Liu, & Tsai, 2001; Chen, Lin, & Lee, 2009; Lee, Chang, Hsu, & Chen, 2011). The designation of zebrafish developmental stages follows that described previously (Kimmel, Ballard, Kimmel, Ullmann, & Schilling, 1995). All animal experiments in this study were performed in accordance with the guidelines issued by the regional animal ethics committee.

2.2. Chemicals and survival rates analysis

All the flavonoids, including flavone, 7-hydroxyflavone, 3,6-dihydroxyflavone, 7,8-dihydroxyflavone, 3′,4′-dihydroxyflavone, 3′,4′,5,7-dihydroxyflavone, 6-methoxyflavone, 7-methoxyflavone, 6-aminoflavone, 7-aminoflavone, chrysin, kaempferol, morin, quercetin, myricetin and rutin (Fig. 1) were purchased from ECHO Chemical Co. (Taipei, Taiwan). All of the chemicals were dissolved in DMSO to the designated concentrations. For the survival rate analysis, 30 embryos were collected and treated with different concentrations of flavonoids for 3 h (72–75 h post-fertilisation (hpf)), and their survival rates were calculated.

2.3. UVB exposure

Embryos that developed to 72 hpf were collected, randomly divided into 30 embryos per experimental group (with or without flavonoids), and exposed to 302 nm UVB generated by a UV cross linker (Spectroline, New York, NY). Each group was exposed to UVB 6 times separated by 30 min intervals (Chen et al., 2011; Wang et al., 2009). Each exposure was around 28 s (100 mJ/cm^2 of energy). After UVB exposure, all embryos were cultivated in 6-well cell culture plates until the analysis of their ROS levels.

2.4. Detection of ROS and data analysis

To detect the accumulation of ROS in zebrafish embryos, embryos from the UVB-only group (no flavonoids added) and embryos from the UVB + 20 ppm flavonoid groups (all flavonoids are listed in Fig. 1) were incubated with 500 ng/ml dihydrodichlorofluorescein diacetate (H2DCFDA, Molecular Probes). Intracellular H2DCFDA was de-esterified to dichlorodihydrofluorescein, which was oxidised by ROS to produce the fluorescent compound dichlorofluorescein (DCF). After a 150-min incubation at 28 °C, the fluorescence intensity of the embryo (FI) was measured at excitation/emission = 485/530 nm. All data were presented as "ROS-scavenging rates" calculated by the following equation: ROS-scavenging rates (%) = (FI$_{flavonoids}$ − FI$_{UVB\ only}$/FI$_{UVB\ only}$) * 100%. FI$_{flavonoids}$ and FI$_{UVB\ only}$ represent the fluorescence intensity (FI) of the UVB + 20 ppm flavonoid group and the UVB-only group, respectively. A positive ROS-scavenging rate means that treatment with the flavonoid compound led to the generation of ROS. A negative ROS-scavenging rate means that the tested flavonoid compound has ROS-scavenging activities.

2.5. Fin-protection experiments

For the fin-protection experiments, embryos at 72 hpf were collected and randomly divided into 5 groups (30 embryos each). In addition to receiving 6 treatments of UVB (100 mJ/cm^2 each), each group was exposed to either water (UVB-only group), water con-
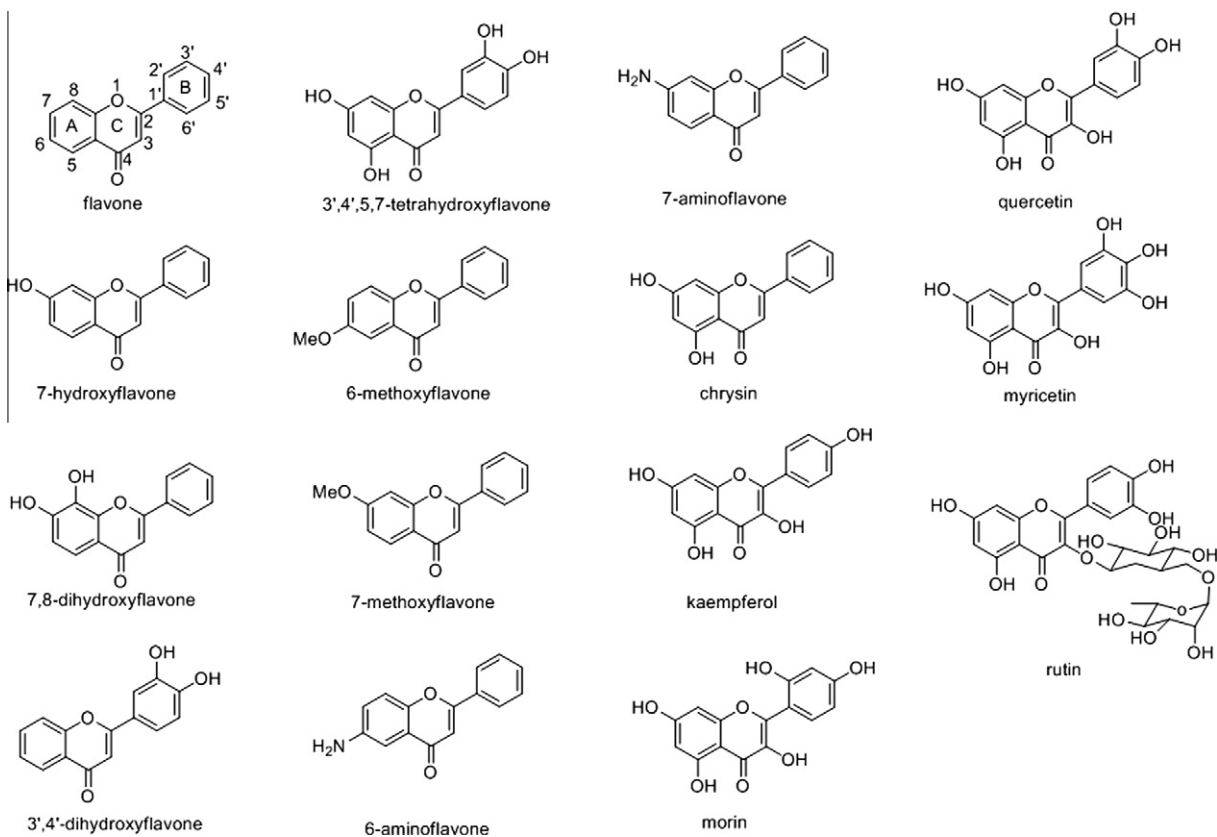

Fig. 1. The structures of flavonoids used in this study.

taining chrysin (10 or 20 ppm), or water containing morin (10 or 20 ppm). The fin malformation rates ((numbers of surviving embryo with malformed fins/30) ∗ 100%) were calculated each day for five days following the UVB exposures.

2.6. Statistical analyses

All analyses in this study were carried out using JMP statistical software (Version 4.02). We treated 'normal fin development' as the event of interest, and regarded embryos that did not achieve normal fin development prior to death or at the end of the experiment as censored data. The Kaplan–Meier method was used to describe the time-to-return phenomena, an estimate of the average time until 'return to normal' occurred for each treatment group. The log-rank test was applied to examine the differences in the malformation (non-return) rates between groups. The Cox proportional hazards fit was employed to quantify the relative probability of normal fin development for each treatment group compared to the control group. A p-value of less than 0.05 was considered statistically significant in all analyses.

2.7. QSAR methods

The 3D chemical structures of all compounds were built initially using Hyperchem, version 6.03 (HYPERCHEM 6.03 Hypercube, http://www.hyper.com) and subsequently exported to Accelrys Discovery Studio, version 2.1 (DS) (Accelrys Inc., San Diego, CA). All geometries were optimised by CHARMM force fields (Discovery Studio. Accelrys Software Inc., Cambridge, MA) (Brooks et al., 1983), and then their energies were minimised using Steepest Descent followed by Conjugate Gradient algorithms with a convergence gradient value of 0.001 kcal/mol. Fourteen flavonoids with definite ROS-scavenging rates were selected for QSAR analyses, and various physicochemical properties were selected as descriptors for initial QSAR construction. 2D and 3D hybrid QSAR studies have been conducted with the structural, topological, spatial, and thermodynamic descriptors of these flavonoids. To develop the QSAR model, the statistical techniques were used with genetic function algorithm (GFA) and partial least squares (PLS). The genetic function approximation algorithm offers a new approach for building the QSAR and quantitative structure–property relationship (QSPR) models. Replacing regression analysis with the GFA algorithm allows the construction of models competitive with or superior to those produced by standard techniques and makes available additional information not provided by other techniques. Unlike most other analysis algorithms, GFA enables multiple models, where the populations of the models are created by evolving random initial models using a genetic algorithm. GFA can build not only linear models but also higher-order polynomials, splines, and other nonlinear functions (Discovery Studio. Accelrys Software Inc.) (Duchowicz, Vitale, Castro, Fernández, & Caballero, 2007).

2.8. Synthesis of a unique flavonoid, 4′-fluoroflavone

All chemicals were commercially available and used without purification except where otherwise stated. The ^{1}H and ^{13}C NMR spectra were recorded on either a Bruker 300 or a Bruker 600 MHz instrument. The chemical shifts were reported in ppm relative to the reference solvents: CDCl$_3$, ^{1}H (7.26), ^{13}C (77.0); DMSO-d_6, ^{1}H (2.49), ^{13}C (39.7). The melting points were determined using an MP-2D apparatus and were not corrected. HRMS was carried out on a model Finnigan MAT 95S.

1-(2-Hydroxy-4,6-dimethoxyphenyl)ethanone (3). Dimethyl sulphate (2.26 g, 23.8 mmol) was added to a solution of 2,4,6-trihydroxyacetophenone (2.0 g, 11.9 mmol) and K$_2$CO$_3$ (3.45 g, 25.0 mmol) in acetone (48 mL). The solution was stirred at ambient

temperate for 18 h. At the end of the reaction time, the solid was removed by filtration. The resulting solution was concentrated and partitioned between ethyl acetate and water. The organic layer was dried (MgSO$_4$), filtered, and concentrated. The solvent was removed and used in the next step without further purification.

2-Acetyl-3,5-dimethoxyphenyl-4-fluorobenzoate (4). 1-Ethyl-3-(3-dimethylaminopropyl)carbodiimide) (EDCI; 5.587 g, 29.14 mmol) and 4-dimethylaminopyridine (DMAP; 0.712 g, 5.83 mmol) were added to a mixture of 3 and 4-fluorobenzoic acid (3.267 g, 23.32 mmol) in CH$_2$Cl$_2$ (130 mL) at 0 °C. The solution was gradually warmed to ambient temperature and stirred for 30 h. The resulting mixture was quenched with NaHCO$_3$ (saturated) and extracted with CH$_2$Cl$_2$. The organic layer was dried (MgSO$_4$) and filtered. Purification by flash column chromatography (230–400 mesh SiO$_2$, hex/EtOAc = 9/1) yielded a white solid. Yield: 86%. Mp = 151.0–153.0 °C. ^{1}H NMR (600 MHz, CDCl$_3$): δ 8.15 (dd, J = 5.5 Hz, 1H), 8.14 (d, J = 5.5 Hz, 1H), 7.15 (t, J = 8.7 Hz, 2H), 6.41 (d, J = 2.3 Hz, 1H), 6.35 (d, J = 2.2 Hz, 1H), 3.86 (s, 3H), 3.82 (s, 3H), 2.47 (s, 3H). ^{13}C NMR (150 MHz, CDCl$_3$): δ 199.1, 166.2 (C–F, J = 253.5 Hz), 164.0, 162.3, 159.3, 149.8, 133.0, 132.9, 125.5, 117.1, 115.8, 115.7, 100.1, 96.7, 55.9, 55.6, 31.9. HRMS (ESI) calculated for C$_{17}$H$_{15}$FO$_5$ ([M+H]$^+$) 319. 0979. Found: 319.0982.

1-(4-Fluorophenyl)3-(2-hydroxy-4,6-dimethoxyphenyl)propane-1,3-dione (5). Potassium hydroxide (0.844 g, 15.05 mmol) was added to a solution of 4 (3.192 g, 10.03 mmol) in pyridine (20 mL). The solution was heated at 50 °C for 2 h. The solution was adjusted to pH 3 with 2 N HCl and extracted with ethyl acetate. The organic layer was dried (MgSO$_4$) and filtered. The mixture was concentrated and used for the next step without purification.

2-(4-Fluorophenyl)-5,7-dimethoxy-4H-chromen-4-one (6). Concentrated sulphuric acid (0.25 mL) was added to a solution of 5 in glacial acetic acid (25 mL) and the mixture was refluxed for 1 h. Next, the mixture was diluted with cold water, extracted with ethyl alcohol and washed with brine. The organic layer was dried (MgSO$_4$) and filtered. Purification by flash column chromatography (230–400 mesh SiO$_2$, hex/EtOAc = 3/1) yielded a red solid. Yield: 45%. Mp: 236.5–238.5 °C. ^{1}H NMR (300 MHz, CDCl$_3$): δ 7.88–7.82 (m, 2H), 7.17 (t, J = 8.5 Hz, 2H), 6.60 (s, 1H), 6.54 (d, J = 2.3 Hz, 1H), 6.37 (d, J = 2.3 Hz, 1H), 3.95 (s, 3H), 3.90 (s, 3H). ^{13}C NMR (150 MHz, CDCl$_3$): δ 177.4, 164.5 (C–F, J = 250.1 Hz), 164.1, 159.7 (C–F, J = 21.0 Hz), 128.1, 128.0, 127.7, 116.2, 116.0, 109.2, 108.8, 96.2, 92.8, 56.4, 55.7. HRMS (ESI) calculated for C$_{17}$H$_{14}$FO$_4$ ([M+H]$^+$) 301.0876. Found: 301.0867.

2-(4-Fluorophenyl)-5,7-dihydroxy-4-H-chromen-4-one (1). A solution of 6 (0.759 g, 2.53 mmol) in 48% aqueous HBr (18 mL) was heated under reflux for 12 h. The mixture was cooled to ambient temperate, diluted with NaHCO$_3$ (saturated), and extracted with ethyl acetate. The organic layer was dried (MgSO$_4$) and filtered. The solution was removed, and the residue was crystallised from a mixture of CH$_2$Cl$_2$:MeOH (3:2) as a yellow–green solid. Yield: 37%. Mp: 289.0–291.0 °C. ^{1}H NMR (600 MHz, d_6-DMSO): δ 12.79 (s, 1H), 8.14 (d, J = 9.0 Hz, 1H), 8.13 (d, J = 9.0 Hz, 1H) 7.40 (t, J = 9.0 Hz, 2H), 6.95 (s, 1H), 6.51 (d, J = 2.2 Hz, 1H), 6.20 (d, J = 2.2 Hz, 1H). ^{13}C NMR (150 MHz, d_6-DMSO): δ181.8, 164.5, 164.2 (C–F, J = 249.0 Hz), 162.2, 157.4, 129.2, 129.1, 127.3, 116.3, 116.2, 105.1, 103.8, 99.0, 94.1. HRMS (ESI) calcd for C$_{15}$H$_{10}$FO$_4$ ([M+H]$^+$) 273.0563. Found: 273.0559.

3. Results and discussion

3.1. Toxicities and antioxidant activities of selected flavonoids

The goal of this study was to find novel flavonoids that had lower toxicities and higher antioxidant activities than flavone. First, we treated zebrafish embryos with different concentrations of 15

different flavonoids (Fig. 1) to determine their LD_{50}. Interestingly, 7-hydoxyflavone, 6-methoxyflavone, 7-methoxyflavone, 7-aminoflavone and kaempferolwere more toxic than flavone (3–27.86 ppm vs. 35 ppm; Table 1). To examine the antioxidant activities of the flavonoids used in this study, we measured their 'ROS-scavenging rates' to determine whether they have the ability to reduce the number of UVB-induced ROS in zebrafish. As shown in Fig. 2, the ROS-scavenging rate of flavone is −68%, indicating that flavone can remove around 68% of the UVB-induced ROS in zebrafish larvae compared to the UVB-only group (without flavone treatment). Most of the flavonoids tested in this study can reduce the amount of UVB-induced ROS in zebrafish larvae (ROS-scavenging rates: −15 to −101%). However, four flavonoids, 7-hydroxyflavone, 7-methoxyflavone, kaempferol and rutin, have a positive ROS-scavenging rate (9–309%), indicating that they can amplify the number of UVB-induced ROS (Fig. 2). Interestingly, chrysin and morin have relatively higher antioxidant activities (ROS-scavenging rates; −99% and −101%) and lower toxicities (LD_{50} > 100 ppm; Table 1) than the rest of the flavonoids tested. Therefore, we decided to further investigate whether chrysin and morin have chemoprotective activities.

3.2. Chrysin and morin are efficient at protecting zebrafish fins from UVB-induced damage

We previously showed that zebrafish fins are very sensitive to UVB exposure (Liao & Chen, 2010; Wang et al., 2009). Therefore, to test the chemoprotective properties of chrysin and morin, 10 or 20 ppm of either were added to zebrafish larvae. In addition, each group received UVB treatment, and the fin malformation phenotypes were recorded. We applied the Kaplan–Meier method to describe the time-to-return phenomena for each experimental group. The malformation (or non-return) rate curve (Kaplan–Meier estimate) for each group is presented in Fig. 3. The mean times of 'return to normal' and their corresponding standard errors are listed in Table 2. The UVB + morin (20 ppm) experimental group had the shortest average time (3.54 days) of 'return to normal', with a standard error of 0.25 days (Table 2). In addition, the estimated fin malformation rates at 5 days after exposure to UVB are as follows: 85.45% for the UVB-only group, 18.52% for the UVB + chrysin (10 ppm) group, 29.09% for the UVB + chrysin (20 ppm) group, 32.14% for the UVB + morin (10 ppm) group, and 12.91% for the UVB + morin (20 ppm) group (Fig. 3). We used the log-rank test to examine the heterogeneity of the malformation rate curves across the groups. There was a significant difference in time-to-return among these groups (p-value < 0.0001), suggesting that the malformation rate curve for the UVB + morin (20 ppm)

experimental group might be significantly different from the UVB-only group.

The results of the Cox proportional hazards fit are shown in Table 3. The relative probabilities of 'return to normal fin' (with corresponding confidence limits) for the UVB + chrysin (10 and 20 ppm) and UVB + morin (10 and 20 ppm) groups compared to the control (UVB-only) group are as follows: 7.93 (2.72–9.60), 6.30 (2.17–26.71), 5.47 (1.86–23.24) and 11.86 (4.09–50.14), respectively. This indicates, for example, that a zebrafish in the chrysin (10 ppm) group is 7.93 times more likely to achieve 'return' than one in the UVB-only group. As shown in Table 2, all relative probabilities are statistically significant and morin (20 ppm) is the most effective flavonoid for repairing damaged fins. On the basis of these observations, we propose that the UV-protective capacities of flavonoids are highly associated with their antioxidant abilities.

3.3. QSAR analysis

Since the 1980s, topological representation of a molecule (the geometrical aspects of molecular structures) has been taken into account when 3D QSAR show significance value on molecular geometry. In this study, 14 flavonoids with definite ROS-scavenging values were derived from the 3D molecule spatial coordinates. The semi-empirical AM1 calculation was performed for the conformation search, and various physicochemical properties were obtained from the QSAR protocol of DS2.1.

The chromone ring is almost planar, yet the interplanar angle between the chromone and the 2-phenyl ring of parent flavonoid is about 6°[v]; this dihedral angle might be affected by substitution on the phenyl rings. In addition, the hydroxyl groups on the chromone and 2-phenyl ring are other factors that we are interested in. For this purpose, various physicochemical properties of the flavonoids were selected as descriptors used for QSAR construction. These properties include 2D (AlogP, molecular_weight, number of hydrogen acceptors, number of hydrogen donors, number of rotatable bonds, molecular surface area, topological descriptors such as Wiener index, Zagreb index,... etc.) and 3D (dipole, shadow indices, molecular volume, molecular surface area,... etc.) parameters.

In order to develop significant QSAR equations, the statistical methods applied were those of GFA and PLS techniques. GFA is derived from the apocalypse of the life evolution and obeyed the concept of evolution via natural selection. As a result, the derived QSAR equations contain four major descriptors, including 2D (numbers of hydrogen bond donors) and 3D descriptors (molecular fractional polar surface area, area of the molecular shadow in the YZ-plane, length of molecule in the Z-axis).

A reliable QSAR model should be validated with some statistical indexes. In order to check the credibility of the models, several parameters were used, such as squared correlation coefficient (R^2), adjusted squared correlation coefficient (Adj-R^2), and F values. Leave-one-out Cross-Validation R^2 (Q^2) was employed to validate the generated QSAR equations. On the basis of our results of the computational analysis (Table 4), Eq. (1) has the highest R^2, Adj-R^2 and Q^2 values. Thus we adopted this equation for the prediction of the ROS-scavenging rates (%).The plot of the observed and predicted ROS-scavenging rates (%) is shown in Fig. 4:

$$N = 14, \quad LOF = 0.36, R^2 = 0.82, Adj\text{-}R^2 = 0.78, Q^2 = 0.63, F = 24.60$$

3.4. Prediction of novel flavonoids with higher antioxidant activities

Among the four QSAR equations presented in Table 4, MFPSA represents the molecular fractional polar surface area, which is

Table 1
Toxicities of different flavonoids in this study.

| Types of flavonoids	Formula	Substituent	$LD_{50(ppm)}$
Flavone	$C_{12}H_{15}O_2$	None	35.00
7-Hydoxyflavone	$C_{15}H_{12}O_3$	7-OH	3.00
7,8-Dihydroxyflavone	$C_{15}H_{12}O_4$	7,8-OH	62.35
3',4'-Dihydroxyflavone	$C_{15}H_{12}O_4$	3',4'-OH	48.33
3',4',5,7-Dihydroxyflavone	$C_{15}H_{10}O_6$	3',4',5,7-OH	50.00
6-Methoxyflavone	$C_{16}H_{12}O_3$	6-OCH$_3$	13.08
7-Methoxyflavone	$C_{16}H_{12}O_3$	7-OCH$_3$	15.79
6-Aminoflavone	$C_{15}H_{11}NO_2$	6-NH$_3$	36.38
7-Aminoflavone	$C_{15}H_{11}NO_2$	7-NH$_3$	22.70
Chrysin	$C_{15}H_{12}O_4$	5,7-OH	>100
Kaempferol	$C_{15}H_{10}O_6$	3,5,7,4'-OH	27.86
Morin	$C_{15}H_{10}O_7$	3,5,7,2',4'-OH	>100
Quercetin	$C_{15}H_{10}O_7$	3,5,7,3',4'-OH	57.92
Myricetin	$C_{15}H_{10}O_8$	3,5,7,3',4',5'-OH	>100
Rutin	$C_{27}H_{30}O_{16}$	5,7,3',4'-OH 3-rutinose	>100
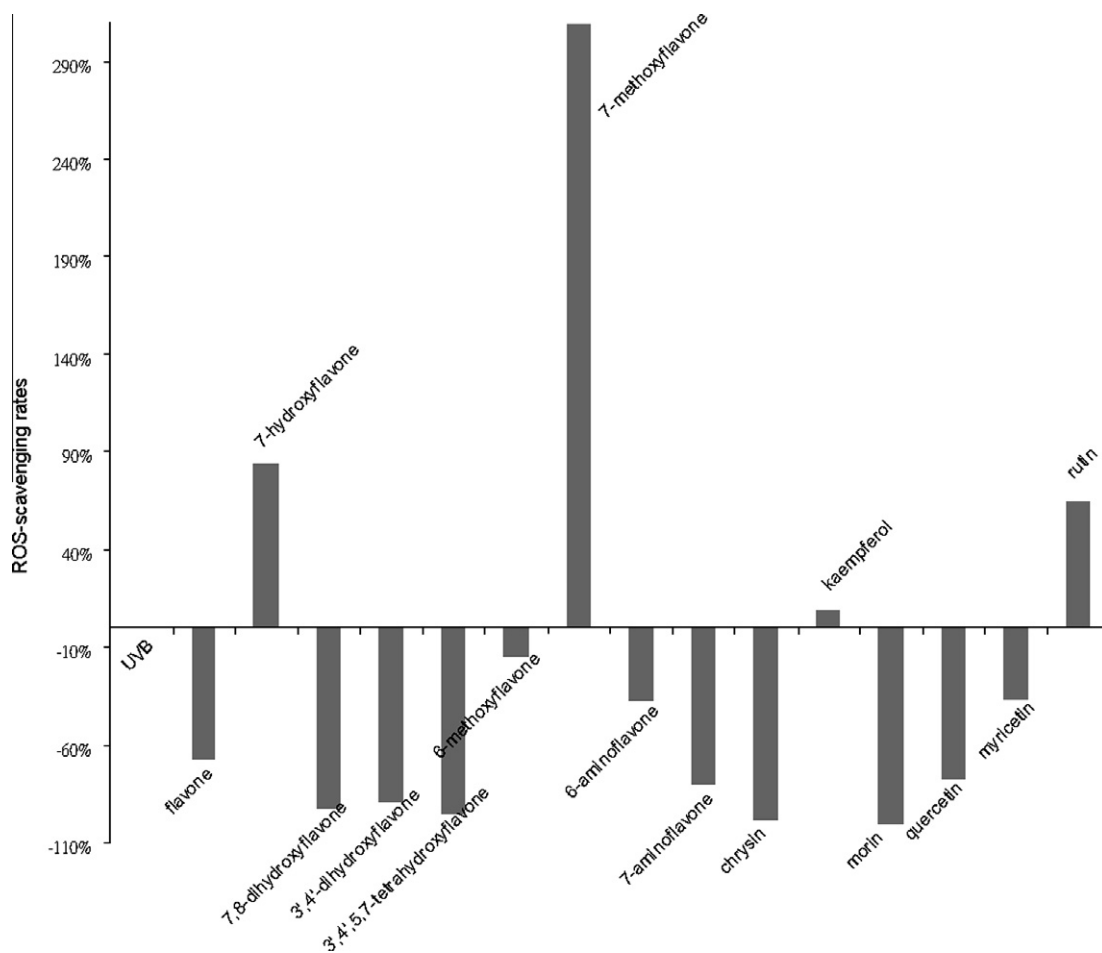
Fig. 2. UV-induced ROS levels are regulated by flavonoids. The ROS levels were measured using the oxidant-sensitive probe, H2DCFDA. The X- and Y-axes represent the different flavonoids and ROS-scavenging rates, respectively. ROS-scavenging rates were calculated using the following equation: ROS-scavenging rates (%) = (FI$_{flavonoids}$ − FI$_{UVB\ only}$/FI$_{UVB\ only}$) ∗ 100%.
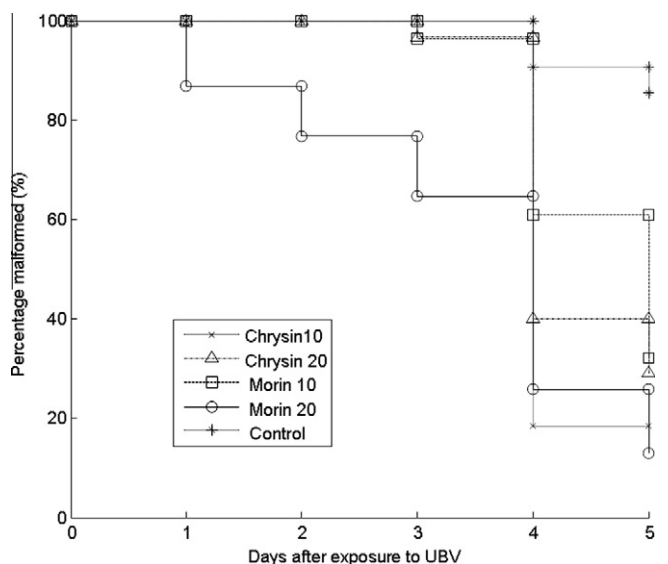

Fig. 3. Kaplan–Meier analysis to determine the number of days required for the pelvic fin of the zebrafish embryos to return to normal following exposure to 10 or 20 ppm of morin or chrysin.

defined as the surface sum over all polar atoms. Molecular shadow indices are a kind of topological descriptor, and the shadow indices of projection represent good correlation between ROS values and

Table 2
Summarised results based on the Kaplan-Meier method for each experimental group: control, morin (10 and 20 ppm), and chrysin (10 and 20 ppm).

Experiment group	Mean time of "return to normal" (day)	Standard error of mean time
Control	4.90	0.08
Chrysin10	4.19	0.00
Chrysin20	4.37	0.10
Morin10	4.57	0.11
Morin20	3.54	0.25

molecular structures. As seen in Table 5, the developed QSAR model also indicates that the ROS-scavenging rates can be intensified by increasing MFPSA and shadow Z length and decreasing shadow YZ values. Based on Eq. (1), there is no sufficient evidence to connect intra-molecular hydrogen bond with ROS value, but the proper positions of substituents may influence the value of Z-plane shadow.

Following the indications of the QSAR equations listed in Table 4, we speculated two compounds and computed their putative antioxidant activities in Table 6.

3.5. Synthesis of a new flavone derivative and its antioxidant activity

Due to the results of the QSAR analysis, we decided to synthesise compound P01 (Table 6). Compound P01 (Flavone 1) was first

Table 3
Cox proportional hazards regression for assessing the effects of treatments on time-to-return.

Experimental group	L–R ChiSquare	p-value	Relative probability	Lower CL	Upper CL
Chrysin10	17.40	0.0000	7.93	2.72	33.65
Chrysin20	13.25	0.0003	6.30	2.17	26.71
Morin10	10.72	0.0011	5.47	1.86	23.24
Morin20	26.60	0.0000	11.86	4.09	50.14

Table 4
QSAR equations to predict the ROS of flavonoids.

No.	QSAR equation	R^2	Adj-R^2	Q^2	F-value
1	$Y = -16.02 + 0.66 * \text{Shadow } YZ - 2.57 * \text{MFPSA} * \text{Shadow } Z \text{ length}$	0.82	0.79	0.63	24.60
2	$Y = -17.34 + 0.65 * \text{Shadow } YZ - 0.18 * \text{NumHBD} * \text{Shadow } Z \text{ length}$	0.81	0.77	0.59	23.29
3	$Y = -6.05 + 0.01 * \text{Shadow } YZ * \text{Shadow } YZ - 2.59 * \text{MFPSA} * \text{Shadow } Z \text{ length}$	0.81	0.77	0.57	22.88
4	$Y = -7.65 + 0.01 * \text{Shadow } YZ * \text{Shadow } YZ \ 0.18 - 160.19 * \text{NumHBD} * \text{Shadow } Z \text{ length}$	0.80	0.76	0.56	22.58

Shadow YZ: Molecular shadow of YZ plane, MFPSA: molecular fractional polar surface area, shadow Z length: molecular shadow of Z-axis length, NumHBD: numbers of hydrogen bond donor.
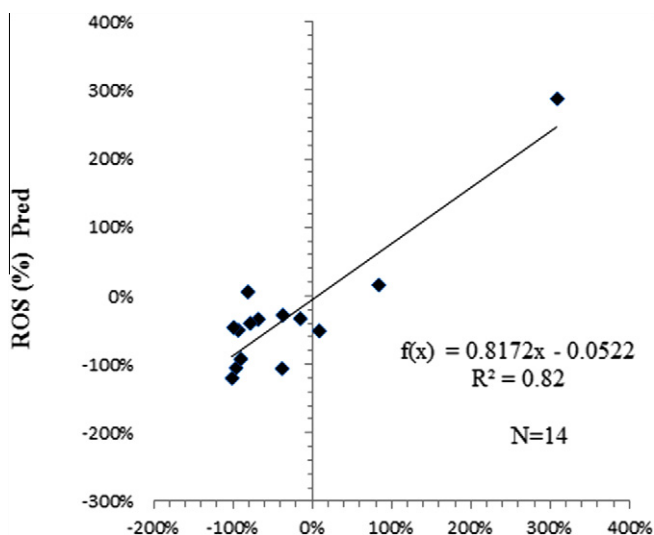
Fig. 4. Plot of observed vs. predicted ROS-scavenging rates (%) of 14 flavonoids.

synthesised in a previous study by a recombinant E. coli system (Katsuyama, Funa, Miyahisa, & Horinouchi, 2007). In this study, we synthesized 1 in a straightforward manner, starting from the commercially available material 2 (Fig. 5). Two hydroxyl groups

of compound 2 were methylated by dimethyl sulphate to give compound 3, which was subsequently coupled with 4-fluorobenzoic acid to yield compound 4. Compound 4 underwent a Baker–Venkataraman rearrangement to give compound 5. Without further purification, compound 5 underwent cyclisation to provide compound 6, which was demethylated by aqueous HBr under refluxing conditions to afford the target molecule compound 1. The overall yield was 15% in five steps from compound 2 (Fig. 5).

In a previous study, flavone 1(2-(4-fluorophenyl)-5,7-dihydroxy-4-H-chromen-4-one) (P01, Table 6), was synthesised in a modified manner, and its ROS-scavenging ability was compared to flavone (Katsuyama et al., 2007). As shown in Fig. 6, the ROS-scavenging rate of molecule 1 is −54%, which corresponds well with the predicted value (−48%) from the QSAR results.

3.6. The positions of hydroxyl and amino groups are associated with the antioxidant activity of flavone

Previous study has been shown that the number of hydroxyl groups and their positions on the A or C rings of flavones are related to their biological activities (Cushman, Nagarathnam, & Geahlen, 1991). Additionally, they synthesised a group of flavones with different hydroxyl group positions and evaluated their LD_{50} compared to that of protein-tyrosine kinases (PKTs). They concluded that at least two hydroxyl groups were necessary to contribute to biological potency. Moreover, they showed that

Table 5
Comparison of ROS-scavenging rates between experimental data and QSAR prediction.

Types of flavonoids	ROS-scavenging rates (%) (experimental data)	Predicted ROS-scavenging rates (Eq. (3)) (%)	MFPSA	NumHBD[a]	Shadow Z length	Shadow YZ
Flavone	−68	−34	0.13	0	4.21	25.87
7-Hydroxyflavone	84	16	0.22	1	4.36	28.16
7,8-Dihydroxyflavone	−93	−50	0.29	2	4.38	28.46
3′,4′,5,7-Tetrahydroxyflavone	−96	−105	0.42	4	4.71	30.34
6-Methoxyflavone	−15	−33	0.15	0	4.29	26.28
7-Methoxyflavone	309	288	0.15	0	4.37	31.18
6-Aminoflavone	−38	−106	0.24	1	4.34	26.65
7-Aminoflavone	−81	6	0.24	1	4.33	28.33
Kaempferol	9	−51	0.42	4	5.69	32.77
Quercetin	−78	−40	0.47	5	6.09	34.89
3′,4′-Dihydroxyflavone	−90	−92	0.29	2	4.55	28.02
Chrysin	−99	−46	0.29	2	4.33	28.59
Morin	−101	−120	0.47	5	5.04	31.73
Myricetin	−37	−28	0.52	6	5.47	34.96

[a] Number of hydrogen bond donor.

Table 6
Theoretical computation of two QSAR-predicted flavonoids.

Predicted compound	MFPSA	NumHBD[a]	Shadow Z length	Shadow YZ	ROS Pred. eq. (1) (%)	ROS Pred. eq. (2) (%)	ROS Pred. eq. (3) (%)	ROS Pred. eq (4) (%)	ROS average (%)
P01	0.28	2	4.37	28.38	−44	−55	−48	−60	−52
P02	0.31	2	4.42	29.11	−31	−9	−39	−16	−24

[a] Number of hydrogen bond donor.
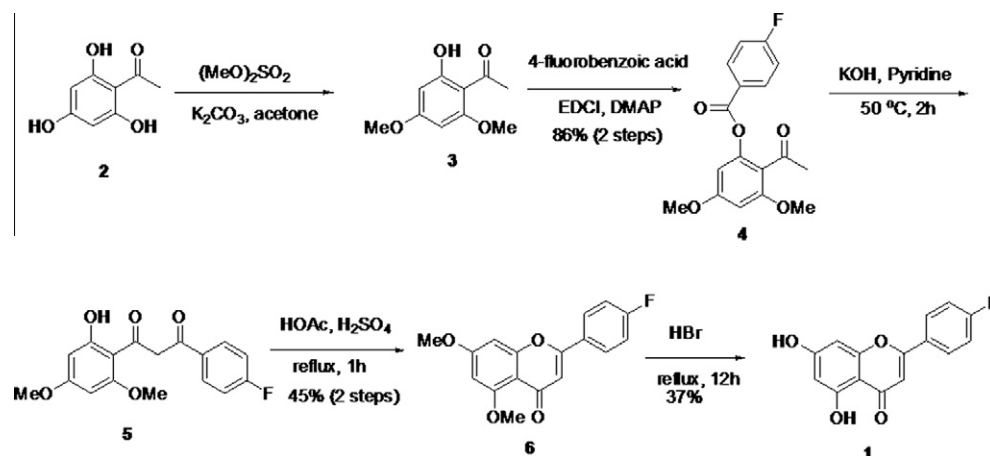
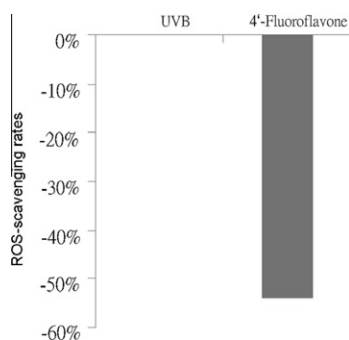**Fig. 5.** Synthesis of a new 4′-fluoroflavone.

Fig. 6. Evaluation of the antioxidant activity of a new flavonoid. The ROS levels were measured using the oxidant-sensitive probe, H2DCFDA.

hydroxyl groups at the C3, C5, and C7 positions of flavones give better results. On the other hand, amino groups that are considered hydrogen donors and acceptors have a similar role to that of hydroxyl groups in flavones (Gao & Kawabata, 2005). Therefore, replacement of hydroxyl groups with amino groups may provide alternative choices for the synthesis of novel amino flavones. However, aminoflavones have been rarely studied or synthesiseduntil recently (Cushman, Zhu, Geahlen, & Kraker, 1994; Dauzonne, Folléas, Martines, & Chabot, 1997; Deng, Lepoivre, & Lemière, 1999; Gao & Kawabata, 2005; Göker et al., 1995; Takechi, Tokikawa, Miyake, & Sasaki, 2006). Lastly, amino groups located at C5 and C4 are better at inhibiting breast cancers (Akama et al., 1996).

4. Conclusion

In this study, we used zebrafish larvae as a model organism to test the antioxidant ability of flavonoids. After comparing the structureactivity relationship of flavonoids and their antioxidant activities by theoretical prediction and experimental methods, several novel compounds were predicted and are ready to be synthesised. This approach is efficient and should be used as a tool for the first round of drug screening.

References

Akama, T., Shida, Y., Sugaya, T., Ishida, H., Gomi, K., & Kasai, M. (1996). Novel 5-aminoflavone derivatives as specific antitumor agents in breast cancer. *Journal of Medicinal Chemistry, 39*, 3461–3496.

Brooks, B. R., Bruccoleri, R. E., Olafson, B. D., States, D. J., Swaminathan, S., & Karplus, M. (1983). CHARMM: A program for macromolecular energy, minimisation, and dynamics calculations. *Journal of Computational Chemistry, 4*, 187–217.

Chang, Y. S., Yang, L. L., & Wang, B. C. (2010). Pharmacophore modeling of tyrosine kinase inhibitors: 4-anilinoquinazoline derivatives. *Journal of the Chinese Chemical Society, 57*, 916–924.

Chen, Y. H., Lee, W. C., Liu, C. F., & Tsai, H. J. (2001). Molecular structure, dynamic expression and promoter analysis of zebrafish (*Daniorerio*) myf-5 gene. *Genesis, 29*, 22–35.

Chen, Y. H., Lin, Y. T., & Lee, G. H. (2009). Novel and unexpected functions of zebrafishCCAAT box binding transcription factor (NF-Y) B subunit during cartilages development. *Bone, 44*, 777–784.

Chen, Y. H., Wen, C. C., Lin, C. Y., Chou, C. Y., Yang, Z. S., & Wang, Y. H. (2011). UV-Induced fin damage in zebrafish as a system for evaluating the chemopreventive potential of broccoli and cauliflower extracts. *Toxicology Mechanisms and Methods, 21*, 63–69.

Chirumbolo, S. (2010). The role of quercetin, flavonols and flavones in modulating inflammatory cell function. *Inflammation Allergy Drug Targets, 9*, 263–285.

Cushman, M., Nagarathnam, D., & Geahlen, R. (1991). Synthesis and evaluation of hydroxylated flavones and related compounds as potential inhibitors of the protein-tyrosine kinase P56[lck]. *Journal of Natural Products, 54*, 1345–1352.

Cushman, M., Zhu, H., Geahlen, R. L., & Kraker, A. J. (1994). Synthesis and biochemical evaluation of a series of aminoflavones as potential inhibitors of protein-tyrosine kinases p56lck, EGFr, and p60v-src. *Journal of Medicinal Chemistry, 37*, 3353–3362.

Dauzonne, D., Folléas, B., Martines, L., & Chabot, G. G. (1997). Synthesis and in vitro cytotoxicity of a series of 3-aminoflavones. *European Journal of Medicinal Chemistry, 32*, 71–82.

Deng, B. L., Lepoivre, J. A., & Lemière, G. (1999). Synthesis of 7-vinylflavone and 7-aminoflavone by palladium-catalyzed coupling reactions. *European Journal of Organic Chemistry, 10*, 2683–2688.

Duchowicz, P. R., Vitale, M. G., Castro, E. A., Fernández, M., & Caballero, J. (2007). QSAR analysis for heterocyclic antifungals. *Bioorganic & Medicinal Chemistry, 15*, 2680–2689.

Gao, H., & Kawabata, J. (2005). α-Glucosidase inhibition of 6-hydroxyflavones. Part 3: Synthesis and evaluation of 2,3,4-trihydroxybenzoyl-containing flavonoid analogs and 6-aminoflavones as α-glucosidase inhibitors. *Bioorganic & Medicinal Chemistry, 13*, 1661–1671.

Göker, H., Ayhan, G., Tunçbilek, M., Ertan, R., Leoncini, G., Garzoglio, R., et al. (1995). Synthesis and antiaggregator activity of some new derivatives of 4H–1-benzopyran-4-one. *European Journal of Medicinal Chemistry, 30*, 561–567.

Harborne, J. B., & Williams, C. A. (2000). Advances in flavonoid research since 1992. *Phytochemistry, 55*, 481–504.

Havsteen, B. H. (2002). The biochemistry and medical significance of flavonoids. *Pharmacology & Therapeutics, 96*, 67–202.

Heim, K. E., Tagliaferro, A. R., & Bobilya, D. J. (2002). Flavonoid antioxidants: chemistry, metabolism and structure–activity relationships. *Journal of Nutritional Biochemistry, 13*, 572–584.

Katsuyama, Y., Funa, N., Miyahisa, I., & Horinouchi, S. (2007). Synthesis of unnatural flavonoids and stilbenes by exploiting the plant biosynthetic pathway in *Escherichia coli. Chemistry & Biology, 14*, 613–621.

Kimmel, C., Ballard, W. W., Kimmel, S. R., Ullmann, B., & Schilling, T.F. (1995). Stages of embryonic development in the zebrafish. *Developmental Dynamics, 203*, 253–310.

Lee, E. R., Kang, Y. J., Kim, J. H., Lee, H. T., & Cho, S. G. (2005). Modulation of apoptosis in HaCaT keratinocytes via differential regulation of ERK signaling pathway by flavonoids. *Journal of Biological Chemistry, 280*, 31498–31507.

Lee, E. R., Kim, J. H., Kang, Y. J., & Cho, S. G. (2007). The anti-apoptotic and anti-oxidant effect of eriodictyol on UV-induced apoptosis in keratinocytes. *Biological & Pharmaceutical Bulletin, 30*, 32–37.

Lee, G. H., Chang, M. Y., Hsu, C. H., & Chen, Y. H. (2011). Essential roles of basic helix–loop–helix transcription factors, Capsulin and Musculin, during craniofacial myogenesis of zebrafish. *Cellular and Molecular Life Sciences, 68*, 4065–4078.

Liao, H. R., Chang, Y. S., Lin, Y. C., Yang, L. L., Chou, Y. M., & Wang, B. C. (2006). QSAR analysis of the lipid peroxidation inhibitory activity with structure and energetic of 36 flavonoids derivatives. *Journal of the Chinese Chemical Society, 53*, 1251–1261.

Liao, Y. F., & Chen, Y. H. (2010). Zebrafish is emerging to be a model to find sun-protective compounds. *Household & Personal Care Today, 4*, 6–8.

Mazur, A., Bayle, D., Lab, C., Rock, E., & Rayssiguier, Y. (1999). Inhibitory effect of procyanidin-rich extracts on LDL oxidation in vitro. *Atherosclerosis, 145*, 421–422.

Ono, M., Yoshida, N., Ishibashi, K., Haratake, M., Arano, Y., Mori, H., et al. (2005). Radioiodinated flavones for in vivo imaging of beta-amyloid plaques in the brain. *Journal of Medicinal Chemistry, 48*, 7253–7260.

Shao, Z. H., Li, C. Q., VandenHoek, T. L., Becker, L. B., Schumacker, P. T., Wu, J. A., Attele, A. S., & Yuan, C. S. (1999). Extract from ScutellariabaicalensisGeorgi attenuates oxidant stress in cardiomyocytes. *Journal of Molecular and Cellular Cardiology, 10*, 1885–1895.

Takechi, A., Tokikawa, H., Miyake, H., & Sasaki, M. (2006). Synthesis of 3-aminof-lavones from 3-hydroxyflavones via 3-tosyloxy- or 3-mesyloxyflavones. *Chemistry Letters, 35*, 128–129.

Tsai, I. T., Yang, Z. S., Lin, Z. Y., Wen, C. C., Cheng, C. C., & Chen, Y. H. (in press). Flavone is efficient to protect zebrafish fins from UV-induced damages. *Drug and Chemical Toxicology*.

Wang, Y. H., Wen, C. C., Yang, Z. S., Cheng, C. C., Tsai, J. N., Ku, C. C., Wu, H. J., & Chen, Y. H. (2009). Development of a whole-organism model to screen new compounds for sun protection. *Marine Biotechnology, 11*, 419–429.